JOURNAL OF OPTOELECTRONICS AND ADVANCED MATERIALS Vol. 9, No. 8, August 2007, p. 2485 - 2492

Intensity redistribution in diffractive pattern due to fractal phase changes

M. MIHAILESCU*, A. M. PREDA, D. COJOC[a], L. PREDA, E. I. SCARLAT[a], I. M. POPESCU
Physics Department, University "Politehnica" of Bucharest, Romania
[a]TASC-NNL-INFM (National Institute for the Physics of Matter) at Elettra Synchrotron Light Source, Lilit Beam-line, Trieste, Italy

In this paper we are analyzing the influence of the non-binary (i.e. multi-level) changes in a fractal phase map (FPM) of a diffractive element (DE) upon the diffracted intensity. The diffraction efficiency dependence on the modified phase shift is presented. The fractal, bi-dimensional structures are obtained on an opto-electronic device: spatial light modulator (SLM). The FPMs were obtained via a recursive algorithm that generates regular gratings with spatial constants obeying a fractal rule. The spatial distribution of the diffracted intensity is exhibiting also a fractal structure. The contrast of the fractal structure in the screen plane increases significantly in some areas and decreases in others, for a selective phase shift in DE plane. The phase shifting rule obeys a non linear dependence of *1/q* type with respect to the fractal stage of growth *q*. We also study the inverse problem which states the logical frame between the self-similar intensity distribution in the screen plane and the corresponding fractal phase map. The results of the numerical evaluation for the spatial intensity distribution of diffraction patterns are compared with those obtained experimentally.

(Received December 8, 2006; accepted June 27, 2007)

Keywords: Diffractive element, Spatial light modulator, Fractal phase map, Diffraction efficiency, Fourier analysis, Non-binary phase change, Intensity redistribution

1. Introduction

The diffractive gratings are largely used for structured beams generators or speckle contrast reduction in laser projectors. Promising devices seem to be the diffractive elements with fractal structure [1].

The concept of a fractal is most often associated with geometrical objects satisfying two criteria: self-similarity and fractional dimensionality. Self-similarity means that an object is composed of sub-units and sub-sub-units on multiple levels that resemble the structure of the whole object [2]. Mathematically, this property should hold on all scales. However, in the real world, there are necessarily lower and upper bounds over which such self-similar behavior applies. The second criterion for a fractal object is that it has a fractional dimension. This requirement distinguishes fractals from Euclidean objects, which have integer dimensions.

The one-dimensional Cantor set was studied like a diffractive grating [3] or like a generator for diffractive lenses [4], [5]. Also the bi-dimensional fractals are analyzed from theoretical consideration about their generation [6] and the speckle fields generated by scattering the coherent incident field using statistical analysis [7]. The diffraction on fractal objects are investigated firstly for amplitude-only transmission function [8] but recently implementation on SLM is done for binary structures [9].

For a non-binary profile of diffractive element the phase can be changed in two distinct cases. The first method is by variation of the depth of the micro-relief for those with grooves and ridges made in transparent material through photolithography or direct laser writing. The second is by variation of the refractive index in liquid crystal displays. In these cases we pass from a binary to a non-binary phase profile. We study bi-dimensional fractal sets: Sierpinski gasket and Sierpinski carpet like a DE on a spatial light modulator which introduces a different fractal space distribution phase shift in coherent incident wave by refractive index variations.

The Sierpinski carpet is described analytically through multiplication of regularly simplest bi-dimensional phase grating with periods which respect a fractal rule. This approach allows us to study the effect in diffractive pattern of the small changes only in one stage of fractal.

In fractals of different stage of growth appears the same shape, but with size decreased with the same scale ξ. If the shapes of each given stage introduce different phase shift for incident wave (controlled through the potential which is applied on each pixel of SLM) a non-binary profile will be reached and the diffractive pattern will be modified in intensity distribution. To study the diffractive pattern in Fraunhoffer approximation for all fractal phase distributions and grating periods, the Fourier analysis and convolution theorem are used. The spatial behavior of diffraction pattern has the self-similar characteristics. The correlation maps in diffractive pattern given by fractal sets with different fractal phase levels is numerically evaluated when the reference is the response of regular black and white fractal set. To make evident the observation about intensity redistribution in diffractive pattern, obtained through fractal phase, we use the coefficients difference of the spatial development of the intensity over the screen plane. In the inverse problem, for a given desired intensity

redistribution between a few peaks, a corresponding fractal phase map is numerically reconstructed.

2. Theory

The optical effect of a diffractive structure characterized by the bi-dimensional transmittance function in the DE plane, with the coordinates (x, y)

$$t(x,y) = A(x,y)\exp\left[i\varphi(x,y)\right] \tag{1}$$

is the generation of the corresponding diffracted waves in the screen plane, with the coordinates $(\tilde{x},\tilde{y})$. When the DE is illuminated by a monochromatic, unit amplitude plane wave, one has, in the far field, the Fraunhofer diffraction pattern given by [10]:

$$T(\tilde{x},\tilde{y}) = \left\{\mathcal{F}\left(t(x,y)\right)\right\}\frac{\exp(ikz)}{iz\lambda}\exp\frac{ik(\tilde{x}^2+\tilde{y}^2)}{2z} \tag{2}$$

where z is the distance between the DE plane and the screen plane, k is the wave number, λ is the wavelength of the incident radiation, and $\mathcal{F}$ is the Fourier transform depending on the spatial frequencies: $f_{\tilde{x}} = \tilde{x}/\lambda z$ and $f_{\tilde{y}} = \tilde{y}/\lambda z$.

The SLM is generating the refractive index map proportional with $\varphi(x,y)$ of the transmittance function $t(x,y)$ by modulating the extraordinary refractive index over the whole area of pixels via the applied voltage. The voltage is electronically addressable according to the fractal structure. Thus, one can generate a fractal index map which gives in the screen plane the intensity distribution:

$$I(\tilde{x},\tilde{y}) = \left|T(\tilde{x},\tilde{y})\right|^2 \tag{3}$$

The simulations were performed using the built-in MATLAB functions with the discrete variables (m,n) and $(\tilde{m},\tilde{n})$ given by:

$$x = m\cdot\Delta p\ ,\ y = n\cdot\Delta p\ ,$$
$$\tilde{x} = \tilde{m}\cdot\Delta\tilde{p}_x\ ,\ \tilde{y} = \tilde{n}\cdot\Delta\tilde{p}_y\ , \tag{4}$$

where Δp and $\Delta\tilde{p}_x, \Delta\tilde{p}_y$ are the distances between the centers of two neighboring pixels contained in the DE plane (pitch) and in the screen plane respectively. By denoting with M the total number of pixels in both x and $\tilde{x}$ directions, and with N the total number of pixels in y and $\tilde{y}$ directions, it is obvious that $m,\tilde{m} = \overline{1,M}$ and $n,\tilde{n} = \overline{1,N}$ (the points with the coordinate (0, 0) is in the left upper corner of the matrices and the (512, 512) pixel is the center of the matrices). While the pitch Δp in the DE plane is given by the manufacturer (32μm in our experimental setup), the dimensions in the DE plane and the screen plane are related each other by the equations [11]: $M\Delta\tilde{p}_x\Delta p = \lambda z$ $N\Delta\tilde{p}_y\Delta p = \lambda z$.

The power spectrum of the diffracted signal is the Fourier transform of the autocorrelation function. Since the optical power distributed in the order (α,β) is proportional with the coefficients $B_{\alpha,\beta}$ of the spatial development of the intensity over the screen plane, it follows that we have a reliable instrument to compare the redistributed intensity by evaluating the differences of the coefficients $B_{\alpha,\beta}$ after and before the phase change:

$$DI = B_{\alpha,\beta} - \left(B_{\alpha,\beta}\right)_0, \tag{5}$$

where $\left(B_{\alpha,\beta}\right)_0$ is the initial value, for binary phase.

3. Experimental setting

The experimental setup consists of a He-Ne laser, a telescope to enlarge the laser spot and ensure a proper illumination of all area of pixels, a SLM, a CCD situated at distance z=7m, perpendicular to the optical axis and a computer used to apply the DE phase map on the SLM.

The SLM is a twisted nematic liquid crystals display from Sony Model LCX016AL, with 26,6×20mm active area, with a VGA graphic card resolution (800 columns and 600 rows active pixels), 32μm pitch, 200:1 contrast ratio, 60Hz image frame rate, nearly phase only modulation, acceptable response time (~5ms), increased fill factor.

To collect the experimental information, we apply on the SLM the transmittance function $t(x,y)$ like a bi-dimensional (600×800 intercepted pixels) distribution of maximum 8-digit quantization of 256 gray levels in RGB mode. Each of them introduces a different value of the potential V_{rms}, which is electronically addressable on each pixel of the SLM. The applied potential is a linear function of gray levels for our 8-bit video digitizer and drive electronics (the producer gives $V_{\text{rms}} = 0{,}5\text{V}$ for white, $V_{\text{rms}} = 4{,}5\text{V}$ for black). The tilt angle θ of the molecules in each cell depends of the applied voltage [12]:

$$\tan\left(\frac{1}{2}\left(\frac{\pi}{2}-\theta\right)\right) = \exp\left[-\left(\frac{V_{\text{rms}}-V_t}{V_0}\right)\right] \tag{6}$$

where V_t is the threshold voltage below which no tilting of the molecules occurs and V_0 is the excess voltage. The tilting of the LC molecules causes a reduction in the effective extraordinary refractive index:

$$\frac{1}{n_e^2(\theta)} = \frac{\cos^2(\theta)}{n_e^2} + \frac{\sin^2(\theta)}{n_o^2}, \tag{7}$$

where n_e and n_o are the refractive indexes of the extraordinary and ordinary component without the applied voltage. The real phase shift which is seen by the incident wave front of monochromatic, unit amplitude plane wave, is

$$\varphi(\theta) = \frac{2 \cdot \pi \cdot h \cdot (n_e(\theta) - n_O)}{\lambda} - \alpha_O, \quad (8)$$

where h is the thickness of the liquid crystal layer and α_O is the angle between the polarization direction of incident wave and optical axis of SLM. The phase matrix is a fractal map consisting in "gray" phase levels corresponding to Eqs. (6), (7) and (8).

4. Results

4.1 Generating the fractal structures

We have generated fractal structures of the Sierpinski type: gasket and carpet. The first is ranging over 6 stages while the second has only 5 stages of growth. The fractals are generated via a recurrent algorithm that permits the numerical reconstruction of the diffraction patterns and the evaluation of the diffraction efficiency.

To construct the Sierpinski triangle we start with the greatest triangle of the side L_g (Fig.1). This is repeatedly decomposed into $\Gamma_g = 3$ congruent figures, each of them having exactly $1/\xi_g=1/2$ the size of the previous one. If the first triangle (q=0) has area $L_g^{\,2}\sqrt{3}/4$, the white area in the current stage q is given by: $S_g\big|_q = \left(L_g / \xi_g{}^q\right)^2 \left(\Gamma_g\right)^q \sqrt{3}/4$. The fractal dimension is defined like: $D_g = \ln(\Gamma_g)/\ln(\xi_g)$, so it is $\ln 3/\ln 2 = 1{,}58$ and is the same for every stage of growth q. It measures the degree of fractal boundary fragmentation or irregularity over multiple scales.

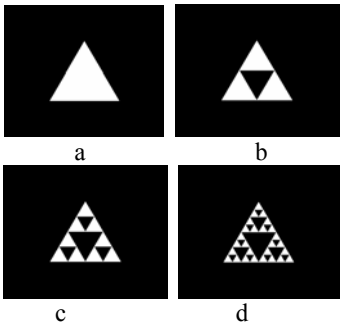

Fig. 1. Phase map applied on SLM for Sierpinski triangle of consecutive stages a) q=0, b) q=1, c) q=2, d) q=3.

To generate the Sierpinski carpet (Fig. 2) we started with a square whose sides have length L_c, following the same algorithm, but with the fractal dimension $D_c = \ln 8/\ln 3 = 1{,}89$. In every stage of growth we obtain a number of $\Gamma_c = 8$ new square of sides length $L_c\big|_q = L_c / \xi_c{}^q$ with $\xi_c = 3$. The white area in the stage of growth q is: $S_c\big|_q = \left(L_c / \xi_c{}^q\right)^2 \left(\Gamma_c\right)^q$.

In Figs 1 and 2, we represent the images of the matrices (0 for black and 1 for white), which generate the phase maps, addressed on SLM.

The transmission function for the bi-dimensional fractal DE – Sierpinski carpet – can be recursively generated starting with a single white square for q=0 on 243×243 pixels. In stage q+1, we obtain the fractal map by multiplying fractal DE from stage q with a regular DE: fractal DE of stage q=2 (Fig. 2c) was obtained by multiplying the fractal DE of stage q−1 (Fig. 2a) with regular DE with period L_c/9 (Fig. 2b) and fractal DE of stage q=3 (Fig. 2e) was obtained by multiplying fractal DE of stage q−1 (Fig. 2c) with regular DE with period L_c/27 (Fig. 2d).

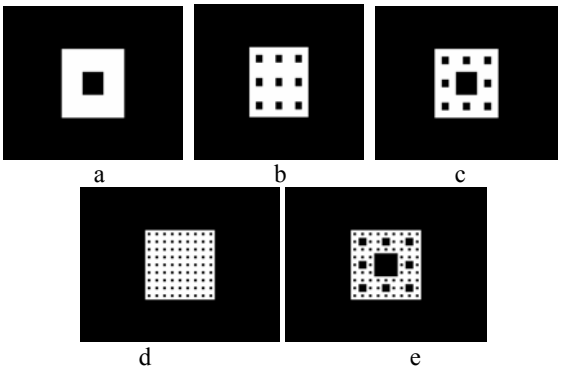

Fig. 2. Sierpinski carpet of consecutive stages a) q=1, c) q=2, e) q=3. In b) and d) are two regular bi-dimensional DE with periods L_c/9 and respectively L_c/27

The binary DEs from Fig.2b and 2d consist of regular distributed squares, white and black. Each of them introduces a phase difference in accordance with Eqs. (6), (7), (8) of the transmitted wavefront: φ_w for white and φ_b for black. The DEs with grooves and ridges can be described analytically by the convolution between the rectangle function and the Dirac delta function [13]. Consequently, the unit cell of a regular DE denoted $t_{\mathrm{ucr}}\big|_q(x,y)$ (see Fig. 3), with the same width (h), but with different refractive indices for φ_w and φ_b, is:

$$t_{\text{ucr}}\Big|_q(x,y) = \sum_{\substack{m,n=1 \\ m=n\neq 2}}^{3}\left[\text{rect}\left(\frac{x}{d_q}\right)\text{rect}\left(\frac{y}{d_q}\right)\right]\otimes$$
$$\otimes\left[\delta(x-\frac{(2m-1)d_q}{2})\delta\left(y-\frac{(2n-1)d_q}{2}\right)\right]e^{i\varphi_w} +$$
$$+\left[\text{rect}\left(\frac{x}{d_q}\right)\text{rect}\left(\frac{y}{d_q}\right)\right]\otimes$$
$$\otimes\left[\delta(x-3\frac{d_q}{2})\delta(y-3\frac{d_q}{2})\right]e^{i\varphi_b} \qquad (9)$$

where $3d_q = L_c / \xi_c^{\,q}$ is the period with fractal properties of the regular grating which generates the fractal in a specific stage q. In the sum of the first term, we didn't take the rectangle with m=n=2. This way to generate the transmission function, simplifies its Fourier transform by using the convolution theorem [10].

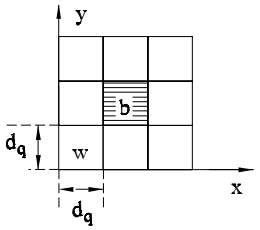

Fig. 3. Unit cell of a 2D regular grating with period $3d_q$

The Fourier transform of the unit cell function forms an envelope function that defines the amplitude and relative phase of each diffracted order. Having defined the transmission function of the unit cell, a 243×243 regular DE can be specified:

$$t_r\Big|_q(x,y) = \sum_{\mu,\nu=1}^{3^{2(q-1)}} t_{ucr}\Big|_q(x,y)\otimes\left[\delta(x-3\mu d_q)\delta(y-3\nu d_q)\right] \qquad (10)$$

Finally, for the stage q, the transmission function will be the product of the regular grating with the period $3d_q$ for transmission function given by (14) and the whole expression of the fractal of stage q−1, so we can recursively write:

$$t(x,y) = \prod_{q=1}^{Q} t_r\Big|_q(x,y) \qquad (11)$$

Here we start with q=1 because for q=0 we have only a white square and the product does not change the final transmission function and we go only at q=5 for the whole active area. We use this expression for t(x, y) in eq. (2) to numerically calculate the diffracted field. Every coefficient from the Fourier decomposition of the transmission function (eq. 11) gives us the diffraction efficiency in corresponding order [13].

4.2 The phase shift influence on the efficiency in the first order: the case of Sierpinski gasket

The pictures of the light distribution in diffractive pattern for the "black" and "white" Sierpinski gasket (q=6) FPM are shown in Fig. 4 (simulated and experimental).

From the theoretical perspective, if the phase of $t(x,y)$ has a fractal structure, it is well known that the Fourier transform preserves fractal properties and the intensity (Fig. 5) in the diffracted pattern will be also self-similar [14,15].

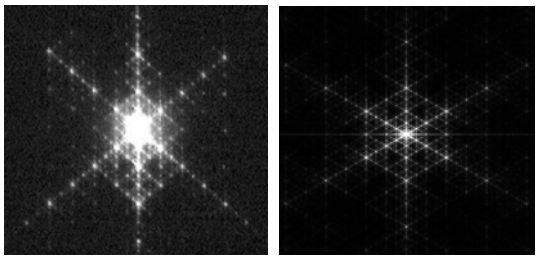

Fig. 4. The experimental a) and simulation b) light distribution in screen plane from Sierpinski gasket with q=6.

Fig. 5. Detail of the experimental picture grabbed on CCD camera and used for box counting fractal dimension In screen plane (Sierpinski gasket, q=6).

By equally shifting the phase from "white" to the same "gray" in all FPM (which had black and gray level) for the stages q=4, 5 and 6, the simulated results are given in Fig.6 (the curved lines). The greater the stage of growth, the greater is the efficiency. The experiment is following the same trend, when the first order efficiency is low due to the smallest difference between phase shift introduced by black and gray.

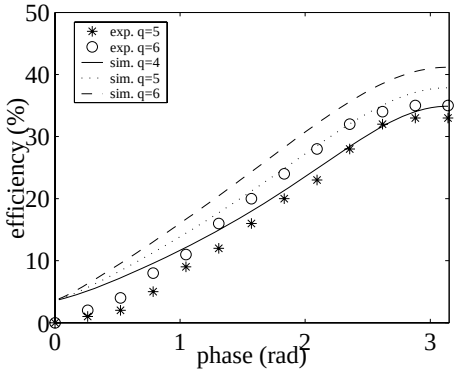

Fig. 6. The efficiency in the first diffracted order: the case of the Sierpinski gasket with uniform phase shift of the "white" levels.

For Sierpinski gasket with binary phase profile, we calculated the diffraction efficiency (simulation) and measured the experimentally one for all stages and we plotted it versus corresponding white area (Fig. 7). The efficiency in diffractive pattern is better at lower grating period (smallest white area) than at higher grating period from DE plane.

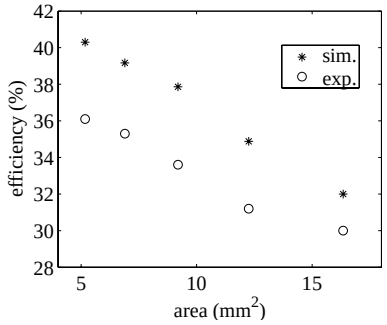

Fig. 7. The diffraction efficiency in first diffraction order experimentally and simulation from Sierpinski gasket with binary phase profile for q = 2, 3, 4, 5, 6 and corresponding white area.

4.3 The selective phase shift influence on the intensity distribution: the case of Sierpinski carpet

For the Sierpinski carpet, the phase is selectively shifted, i.e. we change the "black" level of the FPM with a "gray" level introducing a phase shift according to the following first rule: $\Delta\varphi = \pi / D_c$ for the regular grating with the constant of $3d_1$, … $\Delta\varphi = \pi / 5D_c$, for the regular grating with the constant of $3d_5$ (Fig. 8a). Briefly, the phase shift is

$$\Delta\varphi(q) = \frac{1}{q}\frac{\pi}{D_c}, \tag{12}$$

where q is the stage of growth of the fractal.

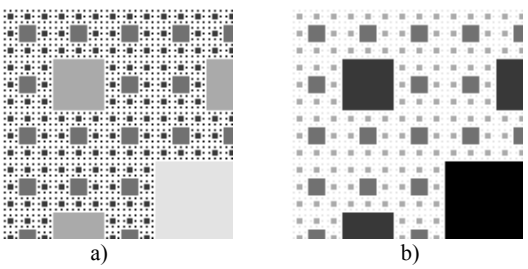

Fig. 8. A quarter of the non-binary fractal like phase map in DE plane with respect of the first selective rule a) and second selective rule b) (Sierpinski carpet, q=5).

The light distribution in the screen plane of this DEs (Fig. 9a) is compared with the one corresponding to the true FPM (i.e. the "black" and "white" fractal, q=5, see Fig. 9b). In figure 9c is the light distribution obtained from non-binary fractal-like phase distribution (Fig. 8b) when we change the "black" level of the FPM with a "gray" level introducing a phase shift according to the following second rule: $\Delta\varphi = \pi / 5D_c$ for the regular grating with the constant of $3d_1$, … $\Delta\varphi = \pi / D_c$, for the regular grating with the constant of $3d_5$.

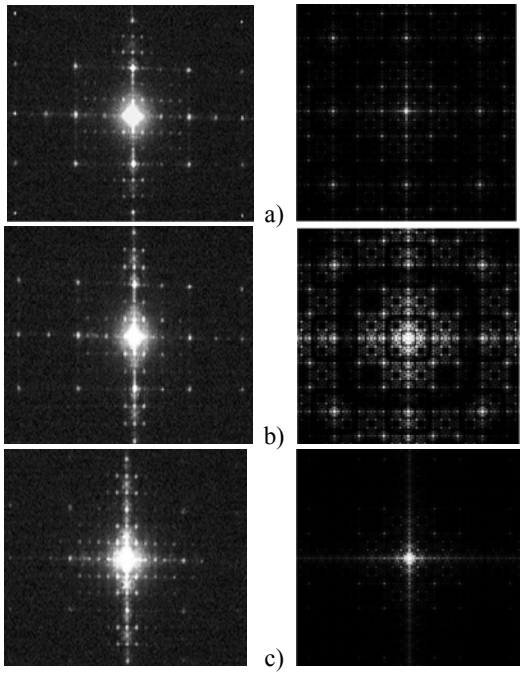

Fig. 9. The experimental (left) and simulated (right) light distribution, for binary phase levels a) for selective phase shift (first rule) b) and for selective phase shift (second rule) c) (Sierpinski carpet, q=5).

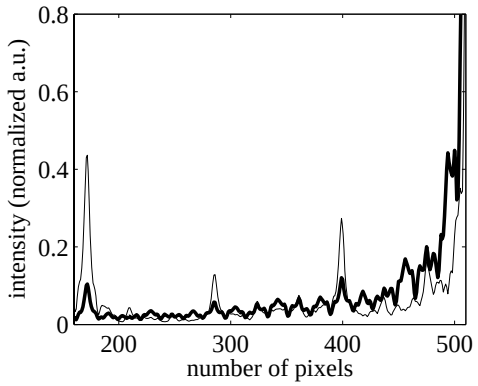

Fig. 10. Cutting portion from the intensity (middle row from the matrix) in screen plane obtained from selective phase shift (first rule) – continuum thin and selective phase shift (second rule) – continuum thick (Sierpinski carpet, q=5).

The sections through the middle row (Fig. 10) for the cases from Figs. 9a and 9c, show us that using the second selective rule for phase in DE plane, the intensity at low frequencies is with 28% higher besides the case when we use the first selective rule. In high frequencies, there is an inverse situation.

We make the correlation map (using the correlation theorem [10]) for simulated intensity distribution between the case from Fig. 9b) and Fig. 9a) and separately from Fig. 9b) and Fig. 9c). We can see that in Fig. 11b) the maximum correlation is at low frequencies. In Fig. 11a) the correlation in central area drastically decreases but correlation exists at high frequencies.

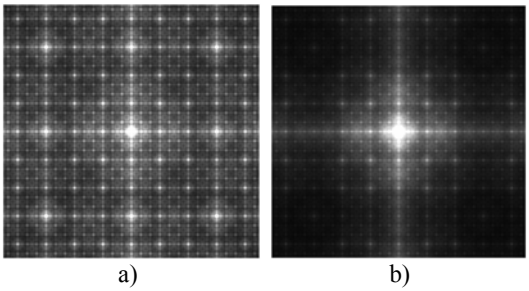

Fig. 11. Correlation map between intensity distribution from a) binary phase map and selective phase shift (first rule) (b) binary phase map and selective phase shift (second rule) (Sierpinski carpet, q=5).

The autocorrelation function is performed for the simulated intensity in the cases from figure 9a and 9c. A cutting portion is shown in Fig.12 (central row of the matrices). Distinguish between the two curves from Fig. 12 is according with the diffractive pattern from Fig. 9a and 9c.

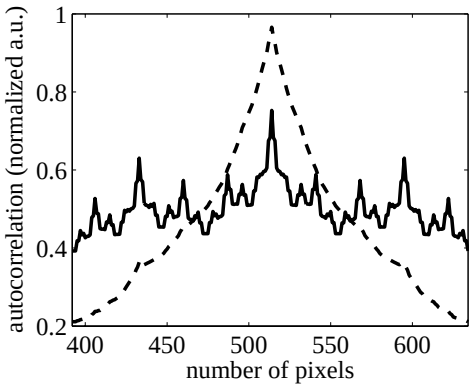

Fig. 12. Cutting portion in autocorrelation function for selective phase shift (first rule) – continuum, and selective phase shift (second rule) – dot (Sierpinski carpet, q=5).

From a quantitative perspective, we use Eq. (5): the intensity redistribution is evaluated as the difference between the experimental distributions given in Fig. 13.

The differences are significant for the odd modes corresponding to the lowest spatial frequencies. Additionally, the fractal structure in screen plane becomes more visible due to the redistribution of the optical energy toward some higher frequencies. The net result is a sharper image of the fractal structure. This is confirmed by the decreasing level of the background signal in the autocorrelation function (Fig. 12), leading to a better contrast of the image. These two manners of phase shifting in the DE plane gave rise to redistribution intensity from central part to the remote peaks of the fractal structure in screen plane.

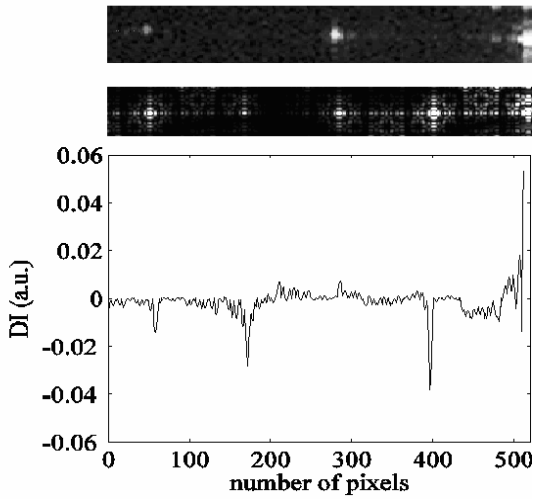

Fig. 13. The experimental redistribution of the optical energy: the intensity for the selective phase shift-(first rule) (uppermost, $\beta = 1$), the intensity for binary phase levels (middle, $\beta = 1$), and the graph of their difference (Sierpinski carpet, q=5).

4.4 The inverse problem

We use our observation about intensity redistribution in the screen plane due to non-binary fractal phase profile in DE plane to change the values of intensity in some specific points.

For a diffractive pattern obtained from a "black" and "white" FPM (Fig 9b), we want to modify the intensity in specific spots. This inverse problem was solved in two distinct cases. In the first case, we apply a (0, 1) band-rejection in the range $\tilde{x},\tilde{y} \in (240,252) \cap (262,274)$ pixel - spatial filtering of the diffractive pattern. In this case, the algorithm for reconstruction has the following steps: we start with a modified intensity pattern (obtained after filtering), and performing an inverse Fourier transform we numerically reconstruct the fractal phase distribution in the DE plane (Fig. 14a). In the reconstruction process, the phase information from screen plane is also used. This procedure brings us changes only in regular grating with period $3d_2$ and the FPM has two levels.

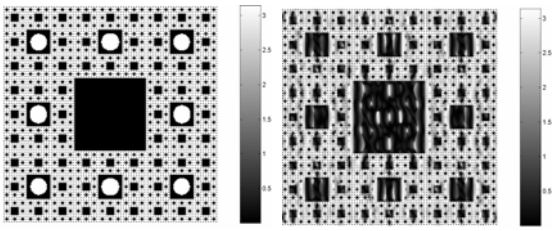

Fig. 14. Phase distribution in the DE plane in a) two levels and b) eight levels.

The second starts with a specific redistribution of the optical intensity in the diffracted space (we change only the value in some peaks, not the spatial distribution). The algorithm is the same, but with different initial intensity pattern. The reconstructed fractal phase map in DE plane was a non-binary one (Fig. 14b). We also must take care at the energy balance in the diffractive pattern after redistribution. The middle row of the intensity distribution in screen plane (cut-off portion) is in Fig. 15 for fractal like phase map from Fig. 14a and 14b. We can see that the intensity has different values at low frequencies.

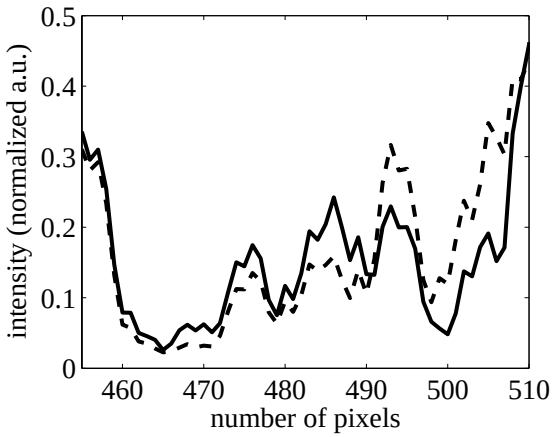

Fig. 15. Intensity in diffractive pattern from fractal-like phase distribution in DE plane from Fig. 14 a) – continuum and from Fig. 14b) – dash.

This result is in concordance with our previous study [16] about Iterative Fourier Transform Algorithm (IFTA). With IFTA we can obtain only the desired intensity in screen plane, the phase in DE plane is incontrollable. But here we can preserve also the phase in DE plane with fractal like structure.

5. Discussion and conclusions

We have recursively generated self-similar sets of Sierpinski carpet form, using regular bi-dimensional grating with the period obeying a fractal rule. The analytical expression for these regular grating was written using the convolution between two simple functions, which simplifies the computation of discrete Fourier transform by using the convolution theorem.

The uniform changes from 0 to π for phase in all white pixels of DE of Sierpinski gasket fractal structure, lead to uniformly increased value for diffraction efficiency deduced by simulation and confirmed experimentally. The diffraction efficiency in the first diffraction order increases with the fractal stage of growth. This effect was explained because of the decreases in the size of the unit cell with different refractive index. The contrast in screen plane increases with the difference between phase shift introduced by black and gray levels of the FPM.

The contrast of the fractal structure in some area of the screen plane increases significantly for a selective phase shift given by a non-binary profile. The phase shifting rule obeys a non linear dependence of $1/q$ type with respect to the fractal stage of growth q. The size of the unit cell, so the period is important in the place where will be formed some intensity peaks but their value depends on the phase shift introduced.

Our observations can be used to increase the intensity in some desired parts of the diffraction pattern and to decrease in others. With this goal, we started with a modified intensity value, but the same spatial distribution in screen plane and through inverse Fourier transform we numerically reconstruct the fractal phase distribution in DE plane. Also the phase information from the screen plane is used. A non-binary fractal phase structure gives us fine steps for intensity in screen plane.

As a result, it was shown that the non-binary fractal phase distribution has a major effect on the intensity in diffractive pattern provided by different DE with the same fractal dimension. The depth of the micro-relief in DE with grooves and ridges or refractive index in DE on SLM can have different values in different points, leading to a non-binary phase levels. Through these gray levels, we can change the values of the intensity but not their spatial distribution. Our observations and conclusions can be applied also for other DE with fractal structure. Our further study is about intensity redistribution through fractal phase changes in lens generated with Cantor set.

References

[1] J. A. Rodrigo, T. Alieva, M. L. Calvo, J. A. Davis, J. of Modern Optics **52**(18), 2771 (2005).
[2] B. Mandelbrot, Freeman, San Francisco, 1982.
[3] Y. Sakurada, J. Uozumi, T. Asakura, Pure Appl. Opt. **1**, 29 (1992).
[4] J. A. Davis, S. P. Sigarlaki, J. M. Craven, M. L. Calvo, Appl. Opt. **45**(6), 1187 (2006).
[5] J. A. Monsoriu, G. Saavedra, W. D. Furlan, Opt. Exp. **12**(18), 4227 (2004).
[6] C. Allain, M. Cloitre, Phys. Rev. B, **33**(5), 3566 (1986).
[7] O. V. Angelsky, P. P. Maksimyak, Meas. Sci. Technol. **9**, 1682 (1998).
[8] B. Hou, G. Xu, W. Wen,G. K. L. Wong, Appl. Phys. Lett. **85**(25), 6125 (2004).
[9] J. A. Davis, L. Martinez, J. A. R. Martin-Romo,

T. Alieva, M. L. Calvo, Opt. Lett. **29**(12), 1321 (2004).
[10] J. W Goodman, Mc Graw-Hill Book Company, 1968.
[11] J. Garcia, D. Mas, R. G. Dorsch, Appl. Opt. **35**, 7013 (1996).
[12] A. Marquez, J. Campos, M. J. Yzuel, I. Moreno, J. A. Davis, C. Iemmi, A. Moreno, A. Robert, Opt. Eng. **39**(12), 3301 (2000).
[13] D. C. O'Shea, T. J. Suleski, A. D. Kathman, D. W. Prather, Spie Press, Bellingham, Washington, USA, 2004.
[14] C. Allain, M. Cloitre, Phys. Rev. A **36**(12), 5751 (1987).
[15] L. Zunino, M. Garavaglia, J. Mod. Opt. **50**(5), 717 (2003).
[16] M. Mihailescu, A. M. Preda, D. Cojoc, E. Scarlat, L. Preda, Intl. Conf. Micro to Nano-Photonics Romopto, Sibiu, Romania, 2006.

*Corresponding author: mona_m@physics.pub.ro